Electronic Supplementary Material (ESI) for Physical Chemistry Chemical Physics.

Supplementary Information

The Synergistic Mechanisms of Apo-Ferritin Structural Transitions and Au(III) ions Transportation: A Molecular Dynamics Simulations with Markov State Model

Xue Peng[1], Chenlin Lu[1], Diannan Lu, Zheng Liu*

State Key Lab of Chemical Engineering, Ministry of Science and Technology

Department of Chemical Engineering, Tsinghua University

Beijing, 100084, China

Corresponding author: ludiannan@tsinghua.edu.cn

Xue Peng and Chenlin Lu contributed equally to the article.

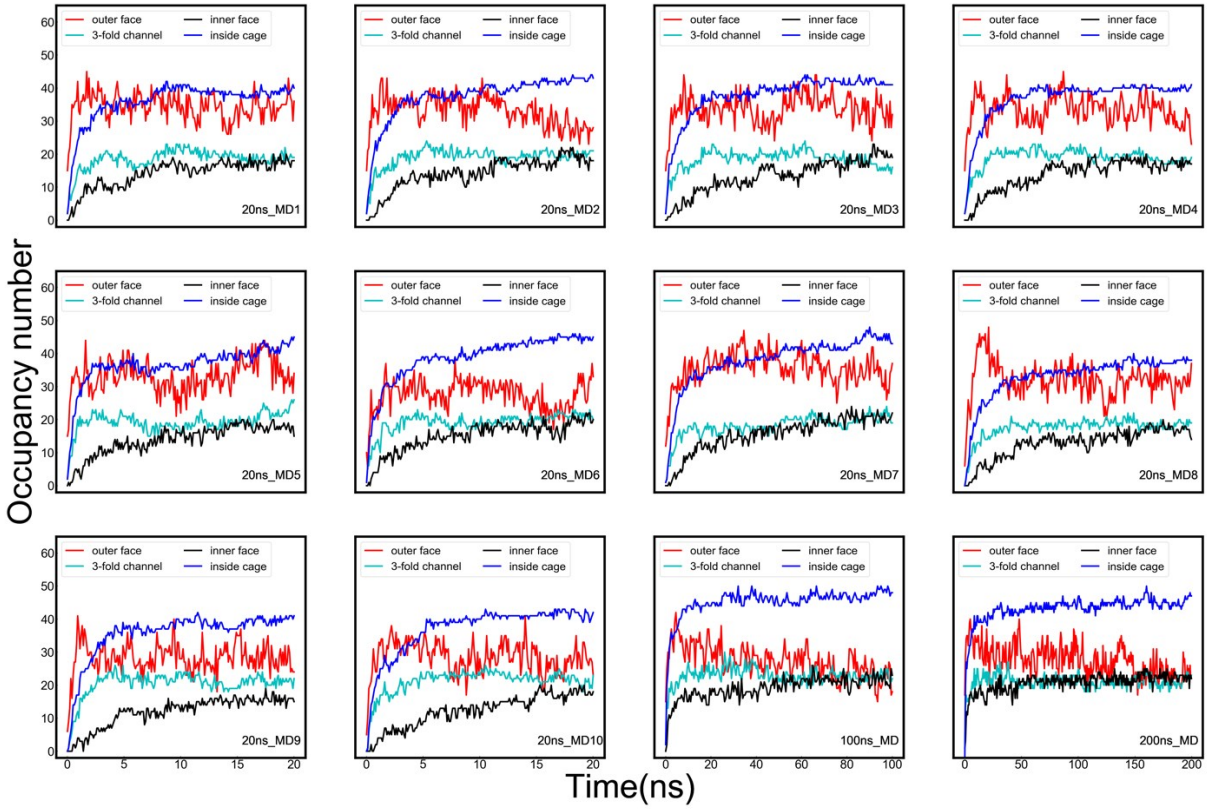

Figure S1. The statistics of the number of Au(III) ions entering the protein cage with the simulation time

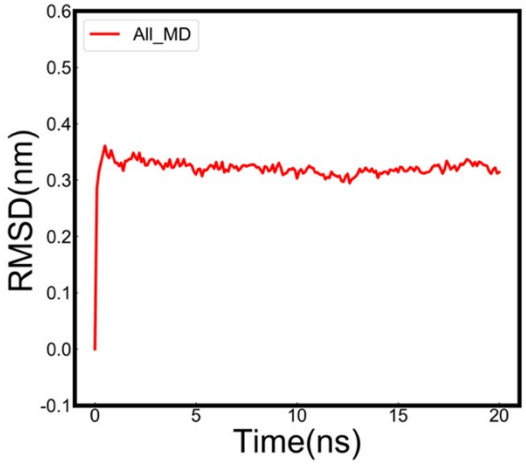

Figure S2. The changes in RMSD of apo-ferritin during the transportation of Au(III) ions

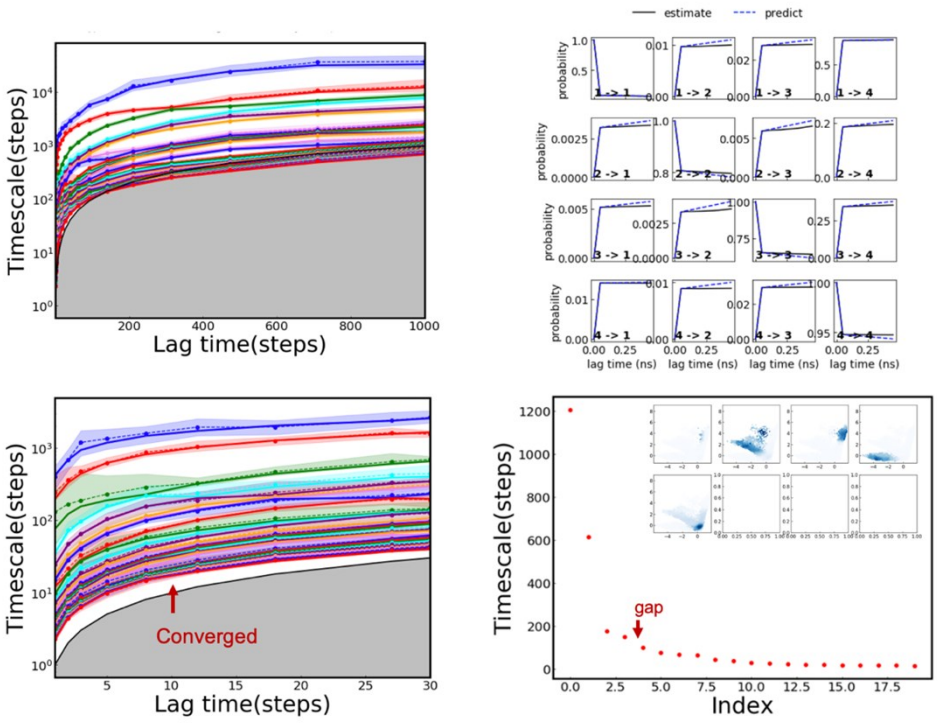

Figure S3. 3-fold MSM construction and validation parameters. The implied timescale plots and the 1σ confidence interval (left). The Chapman–Kolmogorow test of the Markov model (upper-right). Timescales with a gap after the 4th point. (lower-right). The conformational density plots of the five metastable states with PCCA+ algorithm (lower-right, inserted graph).

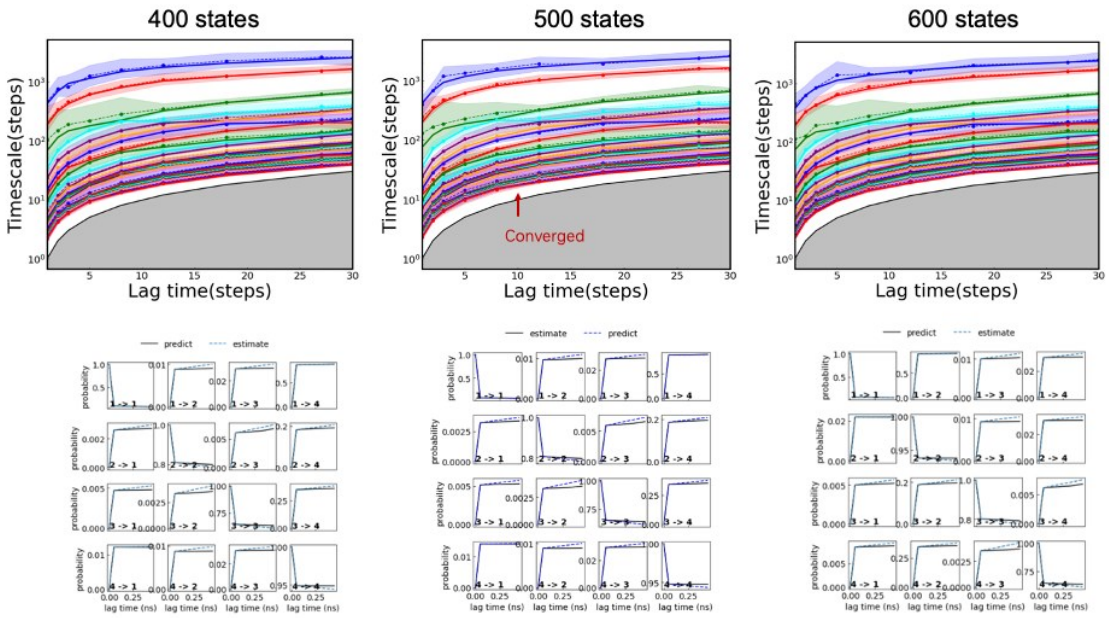

Figure S4. The implied timescale plots and Chapman–Kolmogorow test for 3-fold MSM as a function of different number of microstates, 400 states**,** 500 states**,** and 600 states, respectively.

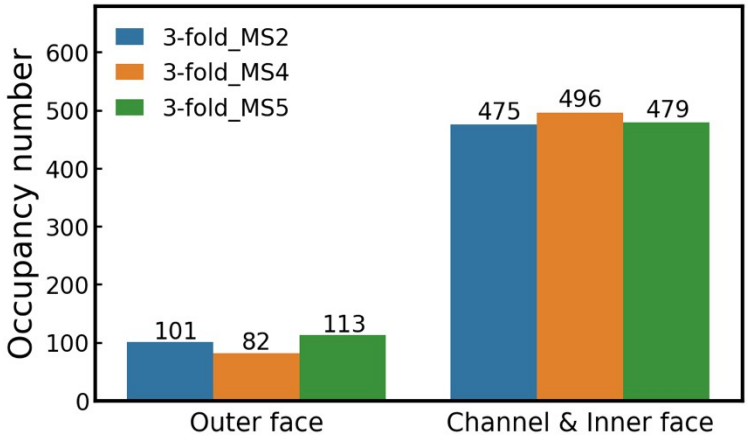

Figure S5. Comparison of the number of residues within 5 Å of Au(III) ions in 3-fold_MS2, 3-fold_MS4 and 3-fold_MS5.

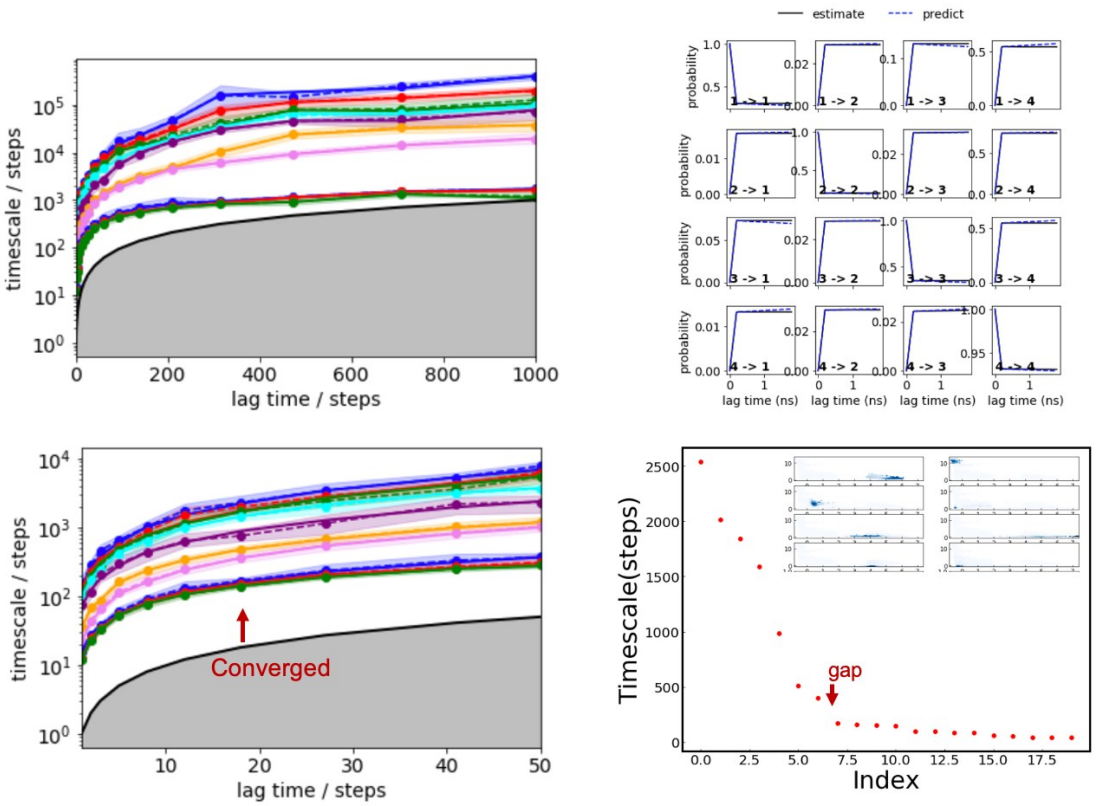

Figure S6. Momober MSM construction and validation parameters. The implied timescale plots and the 1σ confidence interval (left). The Chapman–Kolmogorow test of the Markov model (upper-right). Timescales with a gap after the 7th point. (lower-right). The conformational density plots of the eight metastable states with PCCA+ algorithm (lower-right, inserted graph).

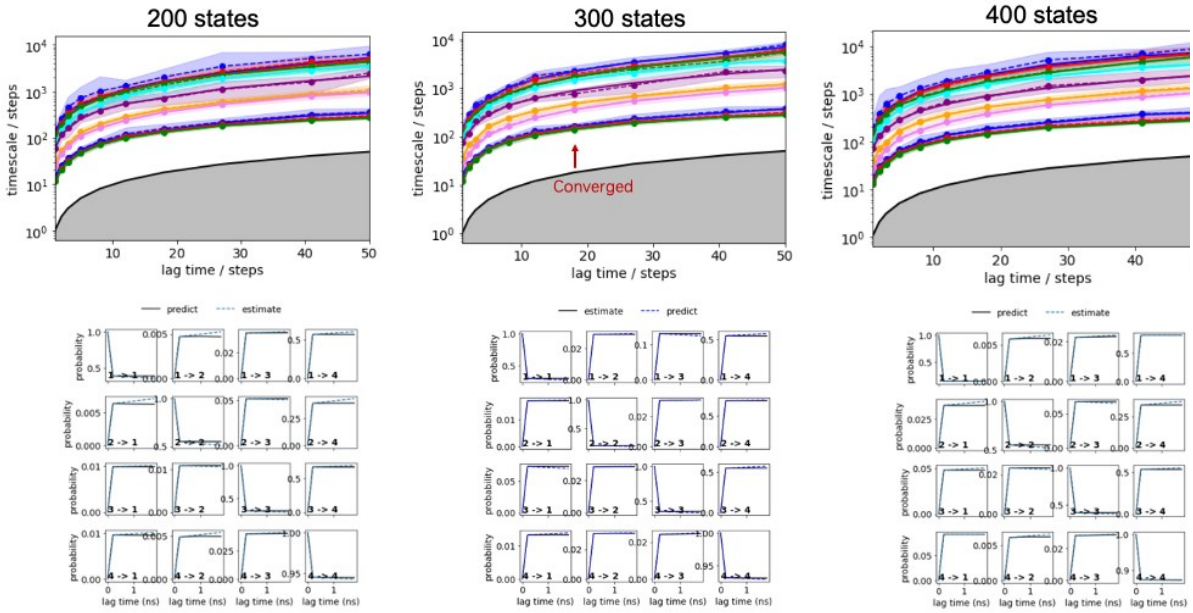

Figure S7. The implied timescale plots and Chapman–Kolmogorow test for momober MSM as a function of different number of microstates, 200 states**,** 300 states**,** and 400 states, respectively.

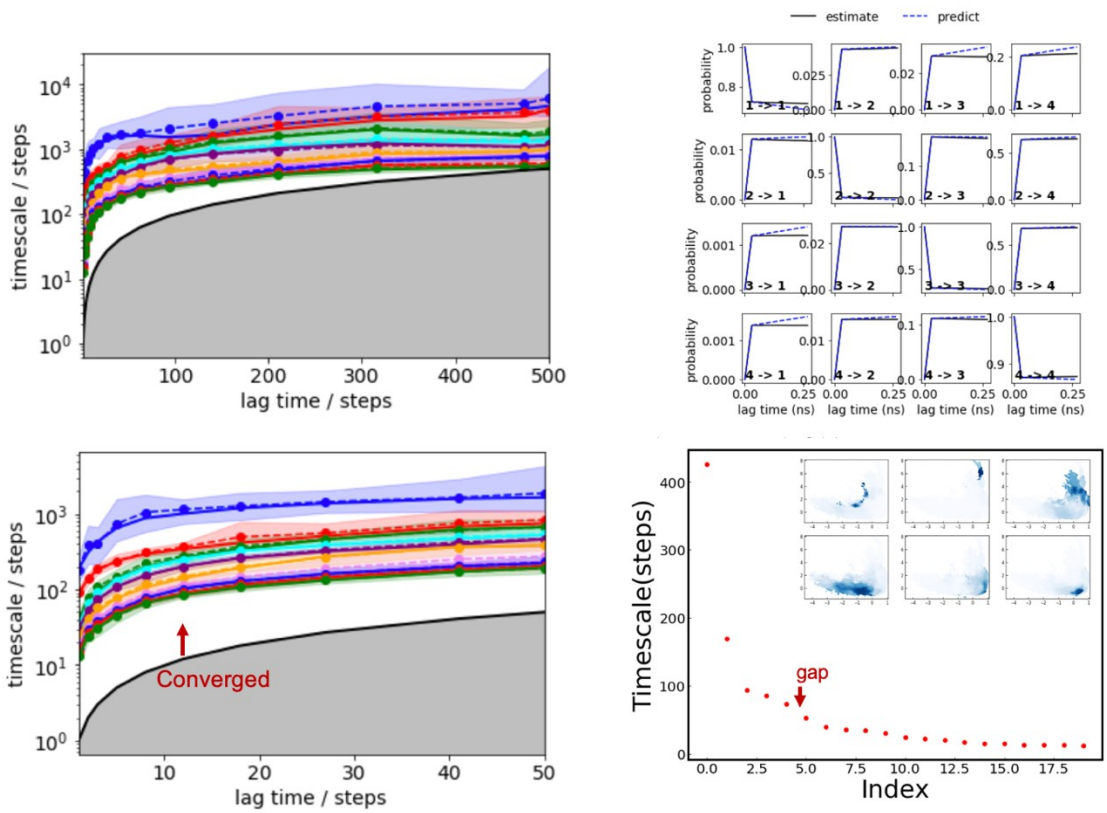

Figure S8. Au MSM construction and validation parameters. The implied timescale plots and the 1σ confidence interval (left). The Chapman–Kolmogorow test of the Markov model (upper-right). Timescales with a gap after the 5th point. (lower-right). The conformational density plots of the six metastable states with PCCA+ algorithm (lower-right, inserted graph).

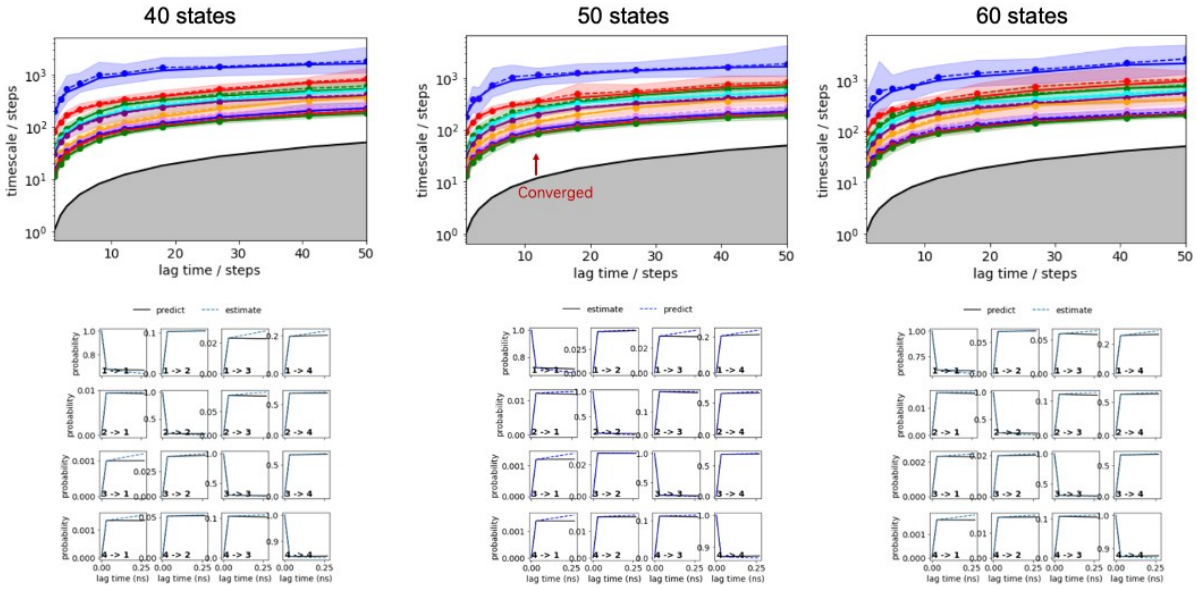

Figure S9. The implied timescale plots and Chapman–Kolmogorow test for Au MSM as a function of different number of microstates, 40 states**,** 50 states**,** and 60 states, respectively.

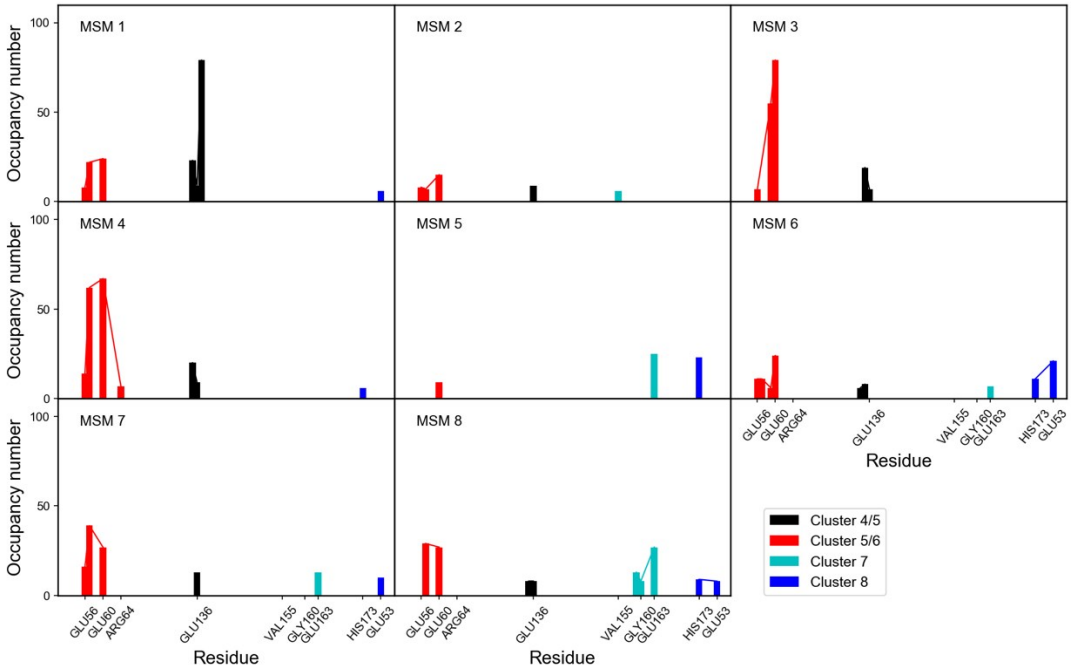

Figure S10. The statistics of the residues within 5A of Au(III) ions in Mono_MS1-8.

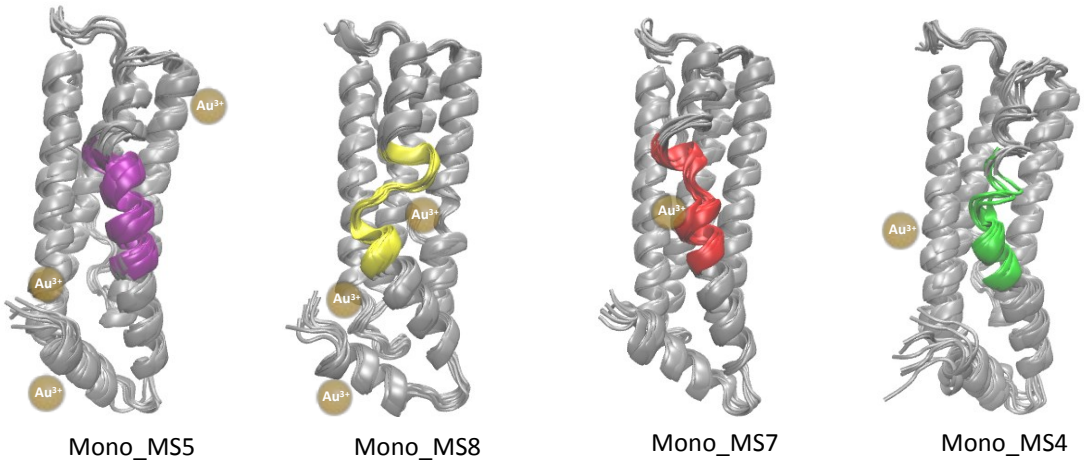

Figure S11. The conformations of four key metasbale states in Monomer MSM and coorsponding Au(III) distribution.

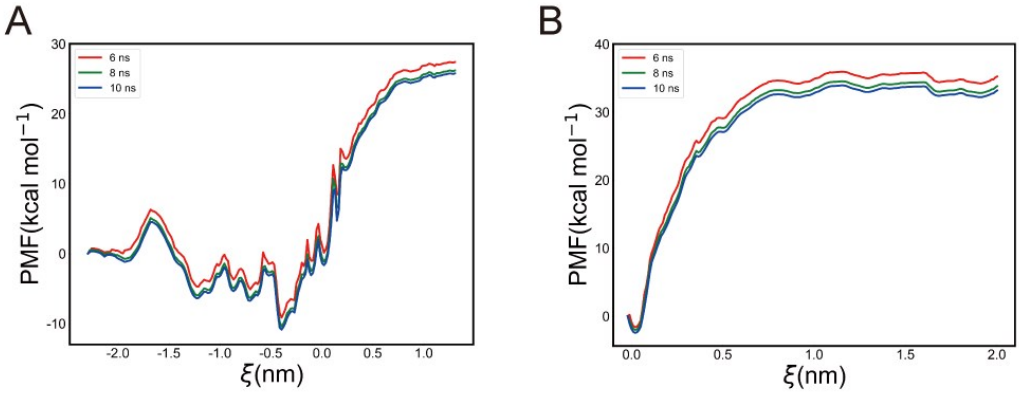

Figure S12. Convergence analysis of PMFs for an Au(III) ion passed through the 3-fold channel and transported to the inner cavity **(A)** or migrated to the inner site **(B)**. As the simulation time per window increased from 6 ns to 10 ns, the PMFs gradually decreased and the PMFs became convergent. In particular, the maximum error between 8 ns and 10 ns does not exceed 0.5 kcal/mol, indicating that the simulation achieves convergent sampling for each window of 10 ns[1,2]. Therefore, the results are discussed with the longest simulation time of 10 ns for each window.

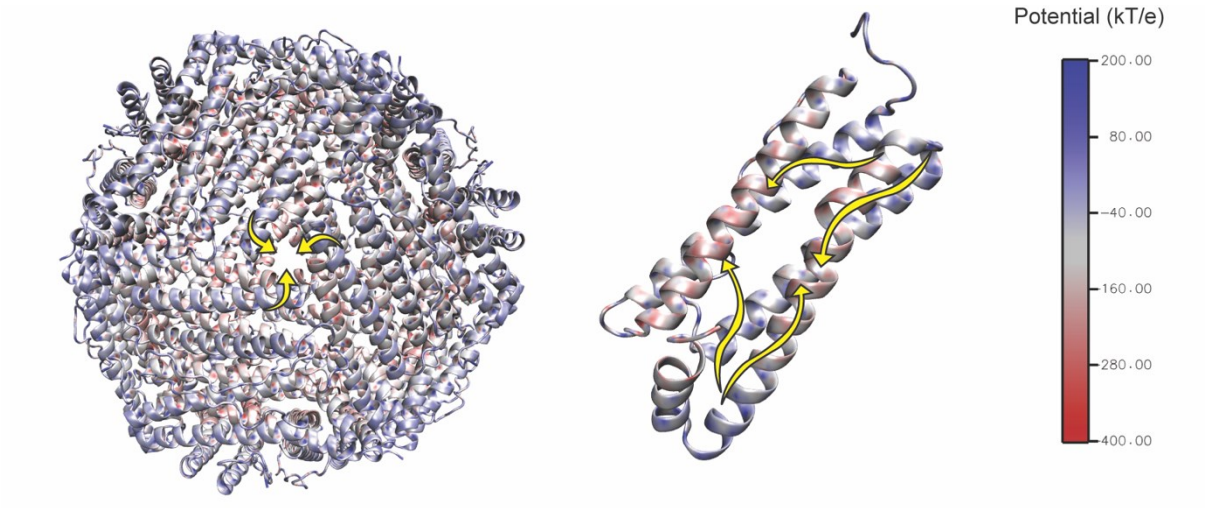

Figure S13. Poisson-Boltzmann electrostatics calculations on the apo-ferritin system, which conducted using PDB2PQR[3] and APBS[4]. The obtained electrostatic potential was visualized on the cartoon model of apo-ferritin by coloring scale (positive: blue; negative: red).

Reference:

[1] Ngo V A, Perissinotti L L, Miranda W, et al. Mapping ryanodine binding sites in the pore cavity of ryanodine receptors[J]. Biophysical journal, 2017, 112(8): 1645-1653.

[2] Wang H, Wang Y, Guo W, et al. Insight into resistance mechanism of anaplastic lymphoma kinase to alectinib and JH-VIII-157-02 caused by G1202R solvent front mutation[J]. Drug design, development and therapy, 2018, 12: 1183.

[3] Dolinsky TJ, Nielsen JE, McCammon JA, Baker NA. PDB2PQR: an automated pipeline for the setup, execution, and analysis of Poisson-Boltzmann electrostatics calculations. Nucleic Acids Research 32 W665-W667 (2004).

[4] Baker NA, Sept D, Joseph S, Holst MJ, McCammon JA. Electrostatics of nanosystems: application to microtubules and the ribosome. Proc. Natl. Acad. Sci. USA 98, 10037-10041 2001.